Preparation of highly luminescent and color tunable carbon nanodots under visible light excitation for in vitro and in vivo bio-imaging

Min Zheng
Beijing Key Laboratory for Green Catalysis and Separation, Department of Chemistry and Chemical Engineering, Beijing University of Technology, Beijing 100124, People's Republic of China; and State Key Laboratory of Luminescence and Applications, Changchun Institute of Optics, Fine Mechanics, and Physics, Chinese Academy of Sciences, Changchun, Jilin 130033, People's Republic of China

Shi Liu, Jing Li, and Zhigang Xie
State Key Laboratory of Polymer Physics and Chemistry, Changchun Institute of Applied Chemistry, Chinese Academy of Sciences, Changchun, Jilin 130022, People's Republic of China

Dan Qu
State Key Laboratory of Luminescence and Applications, Changchun Institute of Optics, Fine Mechanics, and Physics, Chinese Academy of Sciences, Changchun, Jilin 130033, People's Republic of China

Xiang Miao
State Key Laboratory of Luminescence and Applications, Changchun Institute of Optics, Fine Mechanics, and Physics, Chinese Academy of Sciences, Changchun, Jilin 130033, People's Republic of China; and University of Chinese Academy of Sciences, Beijing, People's Republic of China

Xiabin Jing
State Key Laboratory of Polymer Physics and Chemistry, Changchun Institute of Applied Chemistry, Chinese Academy of Sciences, Changchun, Jilin 130022, People's Republic of China

Zaicheng Sun[a)]
Beijing Key Laboratory for Green Catalysis and Separation, Department of Chemistry and Chemical Engineering, Beijing University of Technology, Beijing 100124, People's Republic of China; and State Key Laboratory of Luminescence and Applications, Changchun Institute of Optics, Fine Mechanics, and Physics, Chinese Academy of Sciences, Changchun, Jilin 130033, People's Republic of China

Hongyou Fan[b)]
Center for Micro-Engineered Materials, Department of Chemical and Biological Engineering, University of New Mexico, Albuquerque, NM 87106, USA; and Advanced Materials Laboratory, Sandia National Laboratories, NM 87106, Albuquerque, USA

(Received 31 July 2015; accepted 2 October 2015)

Carbon nanodots (CDs) have generated enormous excitement because of their superiority in water solubility, chemical inertness, low toxicity, ease of functionalization and resistance to photobleaching. Here we report a facile thermal pyrolysis route to prepare CDs with high quantum yield (QY) using citric acid as the carbon source and ethylene diamine derivatives (EDAs) including triethylenetetramine (TETA), tetraethylenepentamine (TEPA) and polyene polyamine (PEPA) as the passivation agents. We find that the CDs prepared from EDAs, such as TETA, TEPA and PEPA, show relatively high photoluminescence (PL) QY (11.4, 10.6, and 9.8%, respectively) at λ_{ex} of 465 nm. The cytotoxicity of the CDs has been investigated through in vitro and in vivo bio-imaging studies. The results indicate that these CDs possess low toxicity and good biocompatibility. The unique properties such as the high PL QY at large excitation wave length and the low toxicity of the resulting CDs make them promising fluorescent nanoprobes for applications in optical bio-imaging and biosensing.

I. INTRODUCTION

Since carbon dots (CDs) were discovered by Scrivens et al.[1]; they, as a new luminescence nanomaterial, have attracted considerable attention due to their potential applications in bio-imaging,[2–5] nanomedicine,[6,7] photocatalyst,[8–12] and light emitting devices.[13–15] Compared with classic quantum dots such as CdSe nanocrystals, CDs possess a series of merits such as, less cost, simple synthesis route, better biocompatibility, lower cytotoxicity, and no blinking fluorescence.[16] Up to date, a variety of techniques have been developed to prepare CDs, mainly including top-down and bottom-up approaches.

Contributing Editor: Winston V. Schoenfeld
Address all correspondence to these authors.
[a)]e-mail: sunzc@bjut.edu.cn
[b)]e-mail: hfan@unm.edu
This paper has been selected as an Invited Feature Paper.
DOI: 10.1557/jmr.2015.323

The top-down methods consist of arc discharge,[1] laser ablation,[17] electrochemical oxidation,[18] and combustion/thermal treatment.[19] The bottom-up routes include microwave,[20] ultrasonic,[21] hydrothermal synthesis,[22–25] and thermal pyrolysis. Among them, the thermal pyrolysis of proper carbon source(s) is a low-cost, efficient and facile technique for large quantity production of CDs. However, the CDs synthesized from thermal pyrolysis method are still limited to their broad applications due to the requirement of UV excitation, emission of a single color (blue), and relatively low QY. UV excitation essentially limits the CD applications in the bio-imaging application due to the low organ penetration depth of UV light. Therefore, visible or IR light excited luminescence is highly desirable for bio-imaging because of the high organ penetration depth. Although CDs show excitation wave length (λ_{ex}) dependent photoluminescence (PL), the intensity and QY of PL rapidly drop down with a high excitation wave length. It is still a challenge to prepare CDs by using bottom-up route with high QY emission under high λ_{ex}.

To obtain high QY luminescent CDs, surface passivation is a vital process. Previous studies suggested that the N-containing diamine-terminated poly-(ethylene glycol) (PEG1500N) played an important role in the surface passivation of CDs.[17] The strong photoluminescent performance of N-containing CDs has a close connection with the introduction of N atoms within the skeleton of carbon nanoparticles.[24,26–28] In synthesis of CDs, citric acid (CA), containing carboxyl groups to facilitate the dehydration and carbonization, is a widely accepted carbon source. CDs showed high quantum yield (QY) using 1,2-ethylenediamine (EDA), as the surface passivation agent.[24,29–31] The EDA has been confirmed to serve dual roles as N-doping precursors and surface passivation agents, both of which considerably enhanced the fluorescence of the CDs.[32–35] However, most of CDs emit light with wide spectrum wavelengths under excitation of UV light, which has a low tissue penetration depth and high background fluorescence when being used in bio-imaging. It is highly desirable to synthesize CDs that emit visible light under excitation of light with large wavelengths such as visible or infrared light.

Herein, we developed a facile thermal pyrolysis route to prepare CDs with high QY using CA as the carbon source and ethylene diamine derivatives (EDAs) including triethylenetetramine (TETA), tetraethylenepentamine (TEPA) and polyene polyamine (PEPA) as passivation agents. The CDs prepared from EDAs, such as TETA, TEPA and PEPA, showed relatively high PL QY (11.4, 10.6, and 9.8%, respectively) under visible light excitation. This is beneficial for the in vivo bio-imaging due to the deep tissue penetration depth compared with UV excitation. With the advantage of low cytotoxicity, great biocompatibility, and tunable multi-color emission under visible light excitation, we investigated these CDs for the first time for in vitro and in vivo bio-imaging. The in vivo bio-imaging experiments revealed that these CDs were stable and can serve as novel fluorescent probes for in vivo imaging by using a wide range of excitation wavelengths.

II. EXPERIMENTAL PROCEDURE

A. CD synthesis

The synthesis was conducted using the method described in our previous work.[31] Typically, a mixture of 2.10 g (10 mmol) of CA and 3.6 g (~35 mmol) of TETA was heated from room temperature to 170 °C and was maintained at 170 °C for 30 min. After naturally cooling to room temperature, acetone was added into the crude products, leading to the precipitation of the CDs. The precipitated CDs were collected by centrifugation. Then the CDs were dialyzed against water for 2 days in a dialysis bag (cutoff Mn: 3.0 kDa) to remove small by-products. The water was replaced every 6 h. Finally the CDs in the dialysis bag were freeze-dried to produce yellow solids.

B. QY measurements

The QYs of the samples were measured in reference to Cumarin 1 (QY 73.0% at 360 nm excitation) and fluorescein (QY 95% at 465 nm excitation). The formula used for QY measurements is as follows:

$$\Phi_X = \Phi_{ST}\left(\frac{Grad_X}{Grad_{ST}}\right)\left(\frac{\eta_X^2}{\eta_{ST}^2}\right) \quad ,$$

where the subscripts ST and X denote standard and test, respectively, Φ is the fluorescence QY, Grad is the gradient from the plot of integrated fluorescence intensity versus absorbance, and η is the refractive index of the solvents used. To minimize the re-absorption effects, absorbance in the 10 mm fluorescence cuvettes should never exceed 0.1 at the excitation wave length.

C. Characterization

Fourier transform infrared (FT-IR) spectra of CDs were recorded as KBr pellets with a Bruker Vertex 70 spectrometer (Bruker, Karlsruhe, Germany) from 4000 to 500 cm^{-1}. Fluorescence emission spectra were recorded on a LS-55 fluorophotometer (Perkin-Elmer Co., Waltham, Massachusetts). UV-Vis absorption spectra were recorded using a Shimadzu UV-2450 spectrophotometer (Shimazdu, Tokyo, Japan). High-resolution transmission electron microscopy (TEM) (HRTEM) images and fast Fourier transform spot diagrams were recorded with a FEI-TECNAI G2 transmission electron microscope (FEI Corporation, Eindhoven, The Netherlands) operating at 200 kV. The crystalline structure was recorded by using an x-ray diffractometer (Bruker AXS D8 Focus; Bruker, Karlsruhe, Germany), using Cu K_α radiation

(λ = 1.54056 Å). X-ray photoelectron spectra were obtained on a Thermo Scientific ESCALAB 250 Multitechnique Surface Analysis instrument (Thermo Fisher Scientific, Hudson, New Hampshire).

D. MTT [3-(4,5-dmethylthiazol-2-yl)-2,5-diphenyltetrazolium bromide] assay cell lines and cell culture

L929 and HepG2 cell lines were purchased from the Institute of Biochemistry and Cell Biology, Chinese Academy of Sciences, Shanghai, China. L929 and HepG2 cells were grown in Dulbecco's modified Eagle's medium (DMEM, GIBCO) supplemented with 10% heat-inactivated fetal bovine serum (GIBCO), 100 U/mL penicillin and 100 μg/mL streptomycin (Sigma), and the culture medium was replaced once very day.

E. Biocompatibility test

L929 cells harvested in a logarithmic growth phase were seeded in 96-well plates with a density of 10^5 cells per well and incubated in DMEM for 24 h. The medium was then replaced by CDs at a final equivalent concentration from 0.32 to 200 μg/mL. The incubation was continued for 48 h. Then, 20 μL of MTT (3-(4,5)-dimethylthiahiazo (-z-y1)-3,5-di-phenytetrazoliumromide) solution in phosphate buffer saline (PBS) with a concentration of 5 mg/mL was added and the plates were incubated for another 4 h at 37 °C, followed by the removal of the culture medium containing MTT and addition of 150 μL of dimethyl sulfoxide (DMSO) to each well to dissolve the formazan crystals formed. Finally, the plates were shaken for 10 min, and the absorbance of the formazan product was measured at 490 nm by using a microplate reader.

F. Cellular uptake

Cellular uptake by HepG2 cells was examined using a confocal laser scanning microscope. HepG2 cells were seeded in 6-well culture plates (a sterile cover slip was put in each well) with a density of 5×10^4 cells per well and allowed to adhere for 24 h. After that, the cells were treated with CDs (5 mg/mL) for 1 h at 37 °C. After that, the supernatant was carefully removed and the cells were washed three times with PBS. Subsequently, the cells were fixed with 800 μL of 4% formaldehyde in each well for 20 min at room temperature and washed twice with PBS again. The slides were mounted and observed with an Olympus FV1000 laser confocal scanning microscope imaging system (Olympus, Tokyo, Japan).

G. In vivo fluorescence imaging

Kunming male mice were obtained from Jilin University, China (56–84 days, 20–25 g) and maintained under required conditions. Their use for this study was approved by the Animal Ethics Committee of Jilin University. Before the subcutaneous injection, the back area of the mouse surrounding the injection point was shaved to minimize autofluorescence. The mouse was subcutaneously injected with CD-TETA, CDs-TEPA and CDs-PEPA (2 mg/mL, 25 μL) at three different places on its back after being anesthetized by intraperitoneal injection of 1% pentobarbital. The mouse was imaged by using a Maestro in vivo optical imaging system (Cambridge Research & Instrumentation, Inc., Woburn, Massachusetts). Various excitations including blue (445–490 nm), green (503–555 nm), and yellow (575–605 nm) light were applied during imaging.

III. RESULTS AND DISCUSSION

A. The morphology and structure of the CDs

The morphology and structure of CDs were confirmed by TEM. Figure 1 shows the TEM results of the CDs-TETA, CDs-TEPA and CDs-PEPA. All CDs show a uniform dispersion without apparent aggregation and an average particle diameter of 3.07 ± 0.43, 3.16 ± 0.53, and 3.73 ± 0.33 nm, respectively. From the HRTEM images [Figs. 1(b), 1(d) and 1(f)], most particles were observed to have a discernible lattice structure. Various lattice planes can be clearly identified with a spacing of 0.21 and 0.245 nm, which correspond to the (103) diffraction plane of diamond-like (sp^3) carbon and (100) facet of graphitic carbon, respectively.

B. The surface components of the CDs

The full survey X-ray photoelectron spectroscopy (XPS) spectra [Figs. 1(g), 1(i) and 1(m)] of CDs-TETA, CDs-TEPA, and CDs-PEPA exhibit three peaks at 285.0, 398.8, and 530.6 eV, which are attributed to C1*s*, N1*s*, and O1*s*, respectively. As shown in Figs. 1(g), 1(i) and 1 (m), the content of nitrogen atoms in CDs was in the sequence of CDs-PEPA > CDs-TEPA > CDs-TETA, indicating that more and more nitrogen atoms were doped into CDs with increasing the nitrogen content in the passivation agents. The high resolution XPS spectra of C1*s* [Fig. 1(h)] can be well deconvoluted into four surface components, corresponding to sp^2 (C=C/C–C) at a binding energy of 284.4 eV, C–N at 285.5 eV, C–O at 287.2 eV, and C=O at 288.3 eV. The high resolution XPS spectrum of N1*s* [Fig. 1(h)] exhibits two peaks at 399.2 and 400.0 eV, relating to N–C and N–H, respectively. FT-IR spectra [Figs. 2(a)–2(c)] were used to identify the surface functional groups present on the CDs. The broad absorption bands at 3000–3500 cm^{-1} are assigned to the stretching vibrations of O–H and N–H, the bands at 1636 and 1210 are attributed to the vibrational absorption band of C=O and Ph–O groups, respectively. While the bands at 1569 and 1311 cm^{-1} are

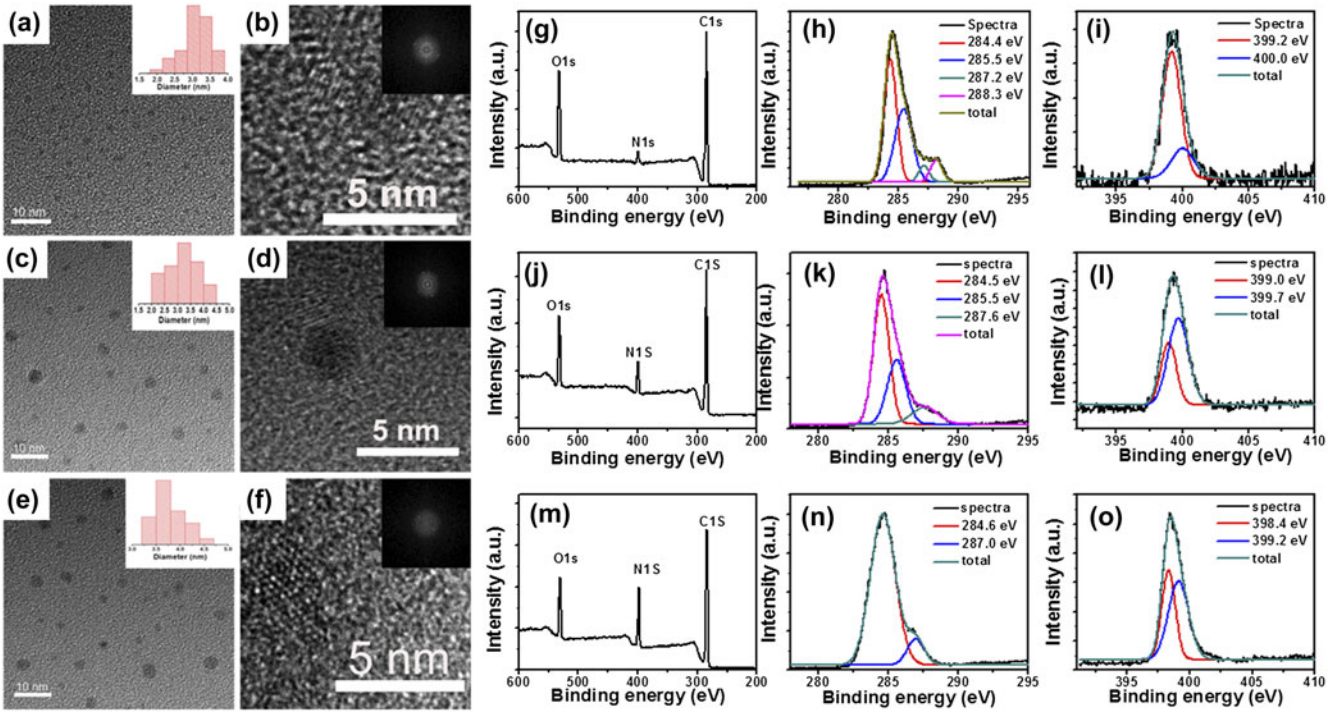

FIG. 1. TEM [left column images (a), (c) and (e)] and HRTEM [right column images (b), (d), and (f)] images of CDs-TETA (a and b), CDs-TEPA (c and d) and CDs-PEPA (e and f). Insets are the corresponding particles size distributions and fast Fourier transform images. XPS (g, j, and m), XPS C1*s* (h, k, and n), and XPS N1*s* (i, l, and o) spectra of CDs-TETA, CDs-TEPA and CDs-PEPA, respectively.

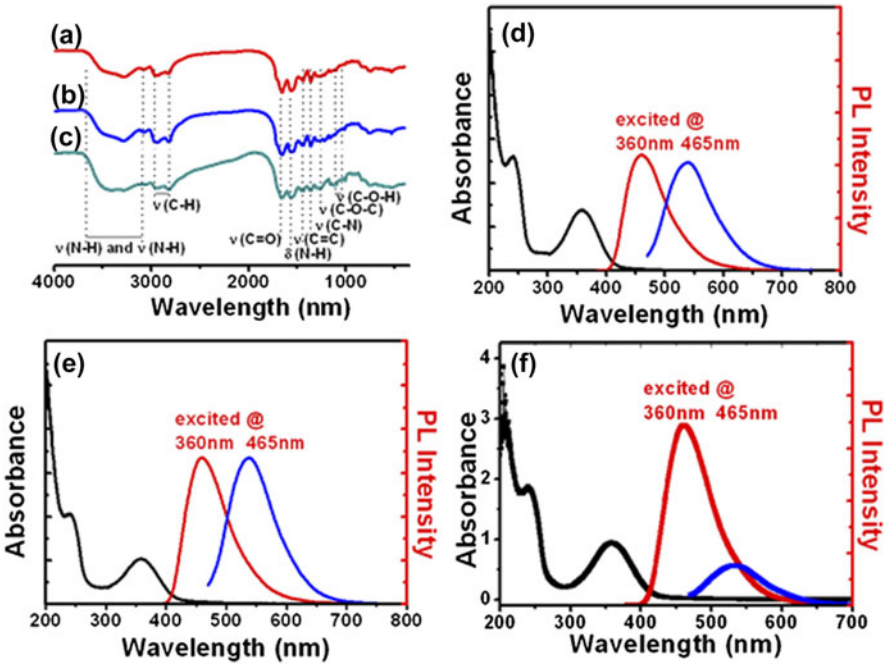

FIG. 2. FT-IR spectra of CDs-TETA (a), CDs-TEPA (b) and CDs-PEPA (c). UV-Vis (black line) and photo-luminescence spectra (red line) of CDs-TETA (d), CDs-TEPA (e), and CDs-PEPA (f).

from the bending vibrations of N–H and C–NH, respectively. These results indicate that there are lots of amino groups on the surface of the CDs. The peaks at 1050 and 1090 cm^{-1} are related to the C–OH stretching vibrations implying the existence of large numbers of hydroxyl groups. The surface chemistry of CDs determined by FT-IR is in good agreement with XPS results. These surface hydroxyl groups are important for the CDs

to disperse in aqueous solutions for their application in the areas of biology and medical science.

C. The optical properties of the CDs

The as-prepared CDs passivated with EDAs exhibit excellent water-soluble properties and excitation-dependent fluorescence emission behavior. The optical characterization results of CDs-TETA, CDs-TEPA, and CDs-PEPA are shown in Figs. 2(d)–2(f). They emit blue luminescence under UV light (365 nm) and green luminescence under blue light (445–490 nm). Cumarin 1 (QY 73.0%) was used as a standard sample to calculate the QY of the CDs, As shown in Table I, the QY is 29.8% for CDs-TETA at 400 nm, 39.0% for CDs-TEPA at 400 nm, and 36.0% for CDs-PEPA at 380 nm. While excited by a visible light, CDs emit relatively bright green, orange and red emissions under the excitation of blue, green, and yellow light, respectively (Fig. 3). For CDs-TETA and CDs-TEPA, the PL intensities excited at 360 and 465 nm are almost the same. When excited at 465 nm, CDs-PEPA displays about a quarter of the maximum emission under an excitation of 360 nm. The PL QY values of CDs-TETA, CDs-TEPA, and CDs-PEPA under excitation of 465 nm are measured to be 11.4, 10.6, and 9.8%, respectively, in reference to fluorescein (QY = 95% at 465 nm excitation, Table I).

D. Biocompatibility of the CDs

Before the CDs were used for bio-imaging in vitro and in vivo, cellular biocompatibility experiments were carried out using the MTT method with L929 as the test cell line. Quantitative analysis of cell viability is shown in Fig. 4. Compared with the blank cells without any other materials added (the survival rate was defined as 100%), the survival rates of L929 coincubated with CDs at six different concentrations all exceeded 75%, indicating that incorporation of CDs does not significantly influence the growth of cells. The MTT assay showed that the CDs possess good biocompatibility and low toxicity that are needed for bio-imaging.

TABLE I. The PL QY of the CDs under the excitation of 400 and 465 nm.

States	CD-TETA		CD-TEPA		CD-PEPA	
λ_{ex} (nm)	400	465	400	465	380	465
$\lambda_{em,max}$ (nm)	466	539	470	539	463	537
Φ_F (%)	29.8	11.4	39.0	10.6	36.0	9.8

E. In vitro and in vivo bio-imaging of the CDs

To validate the multicolor property and imaging application, CDs-TETA, CDs-TEPA, and CDs-PEPA were used as the probes for confocal fluorescence imaging with HepG2 cells. As seen in Fig. 5, after being incubated with CDs-culture solutions, intense blue, green, and red colors were detected under the excitation of 405, 488, and 555 nm, respectively, indicating that these three kinds of CDs are bright for bio-imaging.

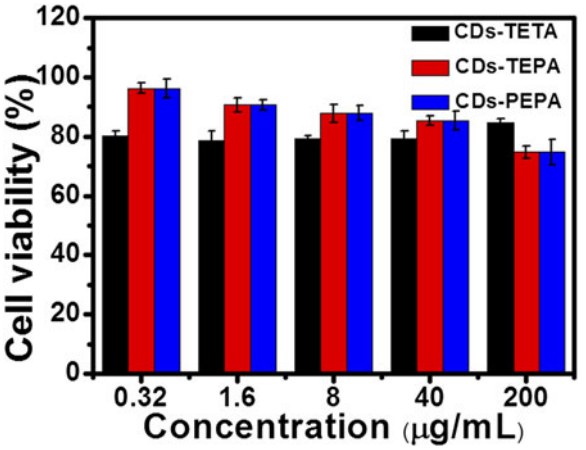

FIG. 4. In vitro biocompatibility of CDs against L929 mouse fibroblast cells in 48 h.

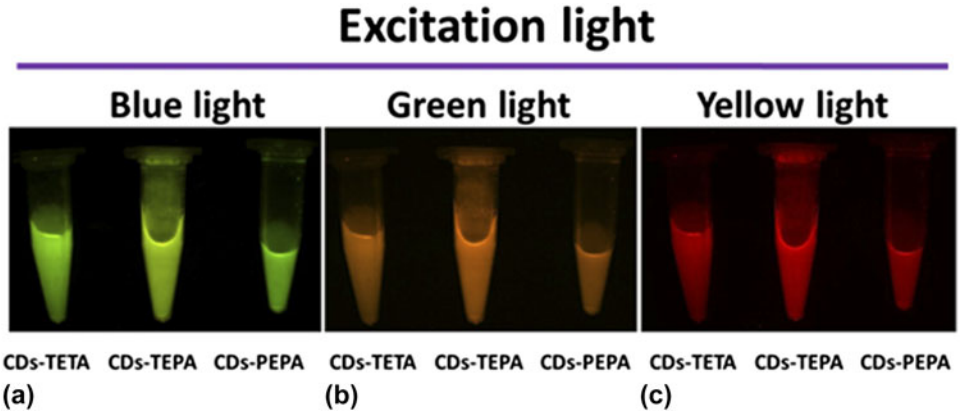

FIG. 3. Fluorescent images of CDs-TETA, CDs-TEPA and CDs-PEPA solutions in the concentration of 5 mg/mL at the excitation of (a) blue light (445–490 nm), exposure time 50 ms and (b) green light (503–555 nm), exposure time 100 ms and (c) yellow light (575–605 nm), exposure time 650 ms.

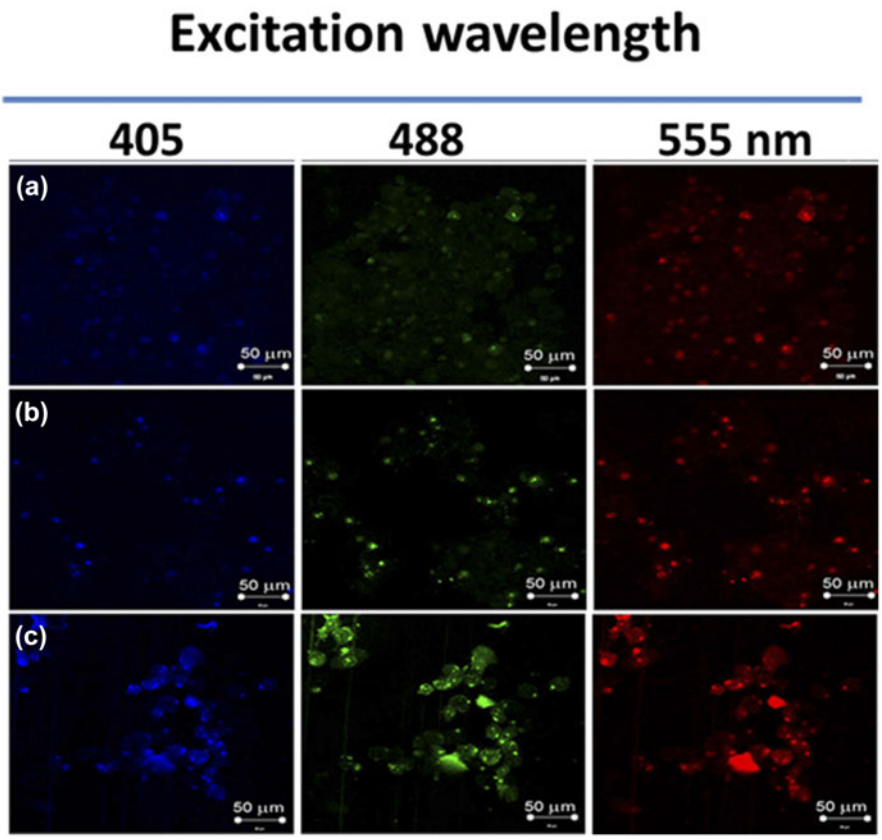

FIG. 5. Laser scanning confocal microscopy images of HepG2 cells labeled with (a) CDs-DETA, (b) CDs-TETA, and (c) CDs-PEPA.

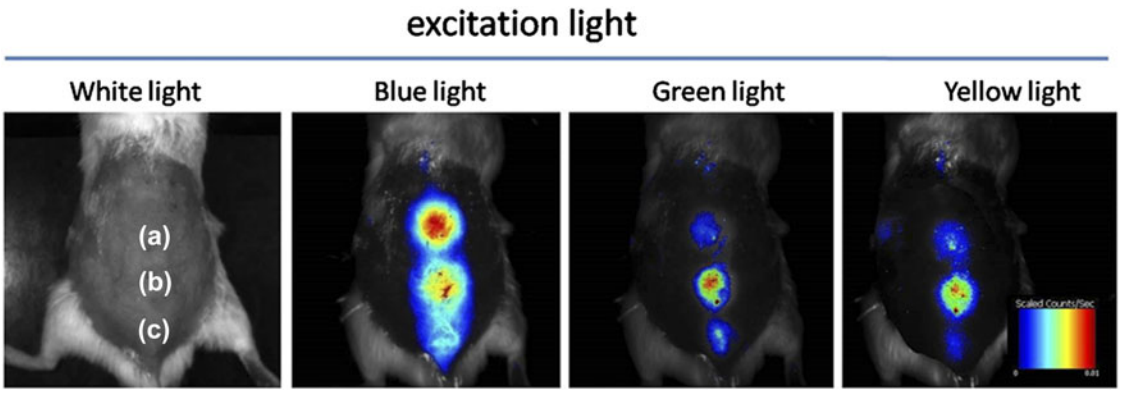

FIG. 6. In vivo fluorescence images of a CD-injected mouse. Spots (a), (b) and (c) represent CDs-TETA, CDs-TEPA, and CDs-PEPA, respectively. The images were taken at different excitation light (blue, green, and yellow).

The CDs were observed mainly in the cell membrane and the cytoplasmic area, especially around the cell nucleus, but the photoluminescence of CDs was very weak in the cell nucleus. With no blinking and low photo bleaching observed, the above laser scanning confocal microscopy studies indicated that these CDs are of remarkably high photostability and biocompatibility for bio-imaging.

Moreover, CDs-TETA, CDs-TEPA, and CDs-PEPA were used for in vivo fluorescence imaging studies in mice. Before the subcutaneous injection, the back area of the mouse surrounding the injection point was shaved to avoid autofluorescence. The mouse was subcutaneously injected with CDs-TETA, CDs-TEPA, and CDs-PEPA (2 mg/mL, 25 μL) at three different places on its back after being anesthetized by a intraperitoneal injection of 1% pentobarbital. And then it was imaged by a Maestro in vivo optical imaging system. Various excitations including blue (445–490 nm), green (503–555 nm), and

yellow (575–605 nm) light were applied during in vivo imaging of the mouse. As shown in Fig. 6, the subcutaneously injected spots of CDs-TETA, CDs-TEPA, and CDs-PEPA on the mouse were seen in the fluorescence images under different excitation lights. The injected CDs in the mouse diffused relatively slowly, and the fluorescence fades gradually in 24 h-post-injection, which is consistent with the previous reports.[35,36]

IV. CONCLUSION

In summary, we have developed a one-step facile route to the synthesis of highly fluorescent CDs using CA as the carbon source and TETA, TEPA, and PEPA as the passivating agents. The synthesized CDs are monodispersive with narrow size distribution. The PL QYs of CDs-TETA, CDs-TEPA, and CDs-PEPA are 11.4, 10.6, and 9.8% under an excitation of 465 nm, respectively. The toxicity studies indicate that the CDs display low toxicity and good biocompatibility. The results from the cell and in vivo imaging indicate that the high QYs along with small particle sizes and low toxicity of CDs-EDAs allow for their wide applications in bio-imaging and biosensing.

ACKNOWLEDGMENT

The project was supported by Open Research Fund of State Key Laboratory of Polymer Physics and Chemistry. The financial support from the National Natural Science Foundation of China (Nos. 21201159, 61176016 and 21104075), Z.S. thanks the support of the "Hundred Talent Program" of CAS, and Innovation and Entrepreneurship Program of Jilin. Z.X. thanks the support of CIAC start-up fund. H.F. acknowledges the support from the U.S. DOE, Office of Basic Energy Sciences, Division of Materials Sciences and Engineering. Sandia is a multiprogram laboratory operated by Sandia Corporation, a wholly owned subsidiary of Lockheed Martin Corporation, for the U.S. Department of Energy's National Nuclear Security Administration under Contract DE-AC04-94AL85000.

REFERENCES

1. X. Xu, R. Ray, Y. Gu, H.J. Ploehn, L. Gearheart, K. Raker, and W.A. Scrivens: Electrophoretic analysis and purification of fluorescent single-walled carbon nanotube fragments. *J. Am. Chem. Soc.* **126**, 12736 (2004).
2. L. Cao, X. Wang, M.J. Meziani, F.S. Lu, H.F. Wang, P.G. Luo, Y. Lin, B.A. Harruff, L.M. Veca, D. Murray, S.Y. Xie, and Y.P. Sun: Carbon dots for multiphoton bioimaging. *J. Am. Chem. Soc.* **129**, 11318 (2007).
3. S.T. Yang, L. Cao, P.G. Luo, F.S. Lu, X. Wang, H.F. Wang, M.J. Meziani, Y.F. Liu, G. Qi, and Y.P. Sun: Carbon dots for optical imaging in vivo. *J. Am. Chem. Soc.* **131**, 11308 (2009).
4. A. Zhu, Q. Qu, X. Shao, B. Kong, and Y. Tian: Carbon-dot-based dual-emission nanohybrid produces a ratiometric fluorescent sensor for in vivo imaging of cellular copper ions. *Angew. Chem., Int. Ed.* **51**, 7185 (2012).
5. D. Qu, M. Zheng, J. Li, Z. Sun, and Z. Xie: Tailoring color emissions from N doped graphene quantum dots for bioimaging applications. *Light: Sci. Appl.* **4**, e364 (2015).
6. P. Huang, J. Lin, X. Wang, Z. Wang, C. Zhang, M. He, K. Wang, F. Chen, Z. Li, G. Shen, D. Cui, and X. Chen: Light-triggered theranostic based on photosensitizer-conjugated carbon dots for simultaneous enhanced-fluorescence imaging and photodynamic therapy. *Adv. Mater.* **24**, 5104 (2014).
7. M. Zheng, S. Liu, J. Li, D. Qu, H. Zhao, X. Guan, X. Hu, Z. Xie, X. Jing, and Z. Sun: Integrating oxaliplatin with highly luminescent carbon dots: An unprecedented theranostic agent for personalized medicine. *Adv. Mater.* **26**, 3554 (2014).
8. H. Li, X. He, Z. Kang, H. Huang, Y. Liu, J. Liu, S. Lian, C.H.A. Tsang, X. Yang, and S.T. Lee: Water-soluble fluorescent carbon quantum dots and photocatalyst design. *Angew. Chem., Int. Ed.* **49**, 4430 (2010).
9. L. Cao, S. Sahu, P. Anilkumar, C.E. Bunker, J.A. Xu, K.A.S. Fernando, P. Wang, E.A. Guliants, K.N. Tackett, and Y.P. Sun: Carbon nanoparticles as visible-light photocatalysts for efficient CO_2 conversion and beyond. *J. Am. Chem. Soc.* **133**, 4754 (2011).
10. H. Ming, Z. Ma, Y. Liu, K. Pan, H. Yu, F. Wang, and Z. Kang: Large scale electrochemical synthesis of high quality carbon nanodots and their photocatalytic property. *Dalton Trans.* **41**, 9526 (2012).
11. J. Liu, Y. Liu, N. Liu, Y. Han, X. Zhang, H. Huang, Y. Lifshitz, S.T. Lee, J. Zhong, and Z. Kang: Metal-free efficient photocatalyst for stable visible water splitting via a two-electron pathway. *Science* **347**, 970–974 (2015).
12. D. Qu, Z. Sun, M. Zheng, J. Li, Y. Zhang, and G. Zhang: Three colors emission from S, N co-doped graphene quantum dots for visible light H_2 production and bioimaging. *Adv. Opt. Mater.* **3**, 360 (2015).
13. X. Guo, C.F. Wang, Z.Y. Yu, L. Chen, and S. Chen: Facile access to versatile fluorescent carbon dots toward light-emitting diodes. *Chem. Commun.* **48**, 2692 (2012).
14. L. Tang, R. Ji, X. Cao, J. Lin, H. Jiang, X. Li, K.S. Teng, C.M. Luk, S. Zeng, J. Hao, and S.P. Lau: Deep ultraviolet photoluminescence of water-soluble self-passivated graphene quantum dots. *ACS Nano* **6**, 5102 (2012).
15. X. Zhang, Y. Zhang, Y. Wang, S. Kalytchuk, S.V. Kershaw, Y. Wang, P. Wang, T. Zhang, Y. Zhao, H. Zhang, T. Cui, Y. Wang, J. Zhao, W.W. Yu, and A.L. Rogach: Color-switchable electroluminescence of carbon dot light-emitting diodes. *ACS Nano* **7**, 11234 (2013).
16. S.N. Baker and G.A. Baker: Luminescent carbon nanodots: Emergent nanolights. *Angew. Chem., Int. Ed.* **49**, 6726 (2010).
17. Y.P. Sun, B. Zhou, Y. Lin, W. Wang, K.A.S. Fernando, P. Pathak, M.J. Meziani, B.A. Harruff, X. Wang, H.F. Wang, P.G. Luo, H. Yang, M.E. Kose, B.L. Chen, L.M. Veca, and S.Y. Xie: Quantum-sized carbon dots for bright and colorful photoluminescence. *J. Am. Chem. Soc.* **128**, 7756 (2006).
18. J. Zhou, C. Booker, R. Li, X. Zhou, T.K. Sham, X. Sun, and Z. Ding: An electrochemical avenue to blue luminescent nanocrystals from multiwalled carbon nanotubes (MWCNTs). *J. Am. Chem. Soc.* **129**, 744 (2007).
19. H. Liu, T. Ye, and C. Mao: Fluorescent carbon nanoparticles derived from candle soot. *Angew. Chem., Int. Ed.* **46**, 6473 (2007).
20. H. Zhu, X. Wang, Y. Li, Z. Wang, F. Yang, and X. Yang: Microwave synthesis of fluorescent carbon nanoparticles with electrochemiluminescence properties. *Chem. Commun.* **34**, 5118 (2009).
21. Z. Ma, H. Ming, H. Huang, Y. Liu, and Z. Kang: Large scale synthesis of carbon nanospheres and their application as electrode

materials for heavy metal ions detection. *New J. Chem.* **36**, 861 (2012).
22. Z.C. Yang, M. Wang, A.M. Yong, S.Y. Wong, X.H. Zhang, H. Tan, A.Y. Chang, X. Li, and J. Wang: Intrinsically fluorescent carbon dots with tunable emission derived from hydrothermal treatment of glucose in the presence of monopotassium phosphate. *Chem. Commun.* **47**, 11615 (2011).
23. S. Liu, J. Tian, L. Wang, Y. Zhang, X. Qin, Y. Luo, A.M. Asiri, A.O. Al-Youbi, and X. Sun: Hydrothermal treatment of grass: A low-cost, green route to nitrogen-doped, carbon-rich, photoluminescent polymer nanodots as an effective fluorescent sensing platform for label-free detection of Cu(II) ions. *Adv. Mater.* **24**, 2037 (2012).
24. S. Zhu, Q. Meng, L. Wang, J. Zhang, Y. Song, H. Jin, K. Zhang, H. Sun, H. Wang, and B. Yang: Highly photoluminescent carbon dots for multicolor patterning, sensors, and bioimaging. *Angew. Chem., Int. Ed.* **52**, 3953 (2013).
25. A.B. Bourlinos, A. Stassinopoulos, D. Anglos, R. Zboril, V. Georgakilas, and E.P. Giannelis: Photoluminescent carbogenic dots. *Chem. Mater.* **20**, 4539 (2008).
26. F. Wang, Z. Xie, H. Zhang, C.Y. Liu, and Y.G. Zhang: Highly luminescent organosilane functionalized carbon dots. *Adv. Funct. Mater.* **21**, 1027 (2011).
27. M.J. Krysmann, A. Kelarakis, P. Dallas, and E.P. Giannelis: Formation mechanism of carbogenic nanoparticles with dual photoluminescence emission. *J. Am. Chem. Soc.* **134**, 747 (2012).
28. C. Liu, P. Zhang, X. Zhai, F. Tian, W. Li, J. Yang, Y. Liu, H. Wang, W. Wang, and W. Liu: Nano-carrier for gene delivery and bioimaging based on carbon dots with PEI-passivation enhanced fluorescence. *Biomaterials* **33**, 3604 (2012).
29. X. Zhai, P. Zhang, C. Liu, T. Bai, W. Li, L. Dai, and W. Liu: Highly luminescent carbon nanodots by microwave-assisted pyrolysis. *Chem. Commun.* **48**, 7955 (2012).
30. L. Tian, D. Ghosh, W. Chen, S. Pradhan, X. Chang, and S. Chen: Nanosized carbon particles from natural gas soot. *Chem. Mater.* **21**, 2803 (2009).
31. M. Zheng, Z. Xie, D. Qu, D. Li, P. Du, X. Jing, and Z. Sun: On–off–on fluorescent carbon dots nanosensor for recognition of chromium (VI) and ascorbic acid based on the inner filter effect. *ACS Appl. Mater. Interfaces* **5**, 13242 (2013).
32. W. Kwon and S.W. Rhee: Facile synthesis of graphitic carbon quantum dots with size tunability and uniformity using reverse micelles. *Chem. Commun.* **48**, 5256 (2012).
33. Q. Dan, M. Zheng, L. Zhang, H. Zhao, Z. Xie, X. Jing, R.E. Haddad, H. Fan, and Z. Sun: Formation mechanism and optimization of highly luminescent N-doped graphene quantum dots. *Sci. Rep.* **4**, 5294 (2014).
34. D. Qu, M. Zheng, P. Du, Y. Zhou, L. Zhang, D. Li, H. Tan, Z. Zhao, Z. Xie, and Z. Sun: Highly luminescent S, N co-doped graphene quantum dots with broad visible absorption bands for visible light photocatalysts. *Nanoscale* **5**, 12272 (2013).
35. P.G. Luo, S. Sahu, S.T. Yang, S.K. Sonkar, J. Wang, H. Wang, G.E. LeCroy, L. Cao, and Y.P. Sun: Carbon "quantum" dots for optical bioimaging. *J. Mater. Chem. B* **1**, 2116 (2013).
36. L. Cao, S.T. Yang, X. Wang, P.G. Luo, J.H. Liu, S. Sahu, and Y. Liu, Y.P. Sun: Competitive performance of carbon "quantum" dots in optical bioimaging. *Theranostics* **2**, 295 (2012).